HemaSphere
Powered by EHA

EHA EUROPEAN HEMATOLOGY ASSOCIATION

Letter

OPEN ACCESS

Extranucleolar CYCLON Staining Pattern Is Strongly Associated to Relapse/Refractory Disease in R-CHOP–treated DLBCL

Antonin Bouroumeau[1,2,*], Lucile Bussot[3], Hervé Sartelet[1], Cyril Fournier[4], Patricia Betton-Fraisse[2], Edwige Col[1], Laurence David-Boudet[1], Anne McLeer[1,2], Christine Lefebvre[2,5], Tatiana Raskovalova[5], Marie-Christine Jacob[5], Claire Vettier[5], Simon Chevalier[5], Caroline Algrin[6], Sylvain Carras[2,3,5], Rémy Gressin[2,3], Mary B. Callanan[4], Thierry Bonnefoix[2,7], Anouk Emadali[2,7]

Correspondence: Anouk Emadali (anouk.emadali@univ-grenoble-alpes.fr); Thierry Bonnefoix (thierry.bonnefoix@univ-grenoble-alpes.fr).

Diffuse large B-cell lymphoma (DLBCL), the most common hematological malignancy in Western countries,[1] is characterized by a high degree of clinical and biological heterogeneity.[2] Current first line therapy consists in an immunochemotherapy regimen referred to as R-CHOP (rituximab, anti-CD20 monoclonal antibody-cyclophosphamide, hydroxydaunorubicine, oncovin, prednisone). Although R-CHOP drastically improved DLBCL outcome,[3] around 10% to 15% of patients exhibit primary refractory disease and an additional 20% to 25% relapse usually within the first 2 years.[3] The revised version of the International Prognostic Index (R-IPI), combining 5 clinical and biological readouts, represents the only robust prognostic factor for DLBCL,[4] but fails to accurately predict these refractory/relapse (R/R) DLBCL cases.

The clinical heterogeneity of DLBCL can be explained by genomic alterations and phenotypic features that include: (1) gene rearrangements involving the proto-oncogene *MYC* and *BCL2*/*BCL6*, defining the high grade B-cell lymphoma (HGBL) formerly referred as "double/triple hit" (DHL/THL) subtype, frequently related to R-CHOP refractory disease,[5] (2) gene expression signatures defining "activated B-cells" or "germinal center" (GC) B-cells DLBCL subtypes, associated with DLBCL prognosis,[6] but not correlated with R-CHOP response, and (3) recently identified recurrent mutational events defining genetic subtypes that could have therapeutic implications.[7,8] But, despite this extensive characterization, no clear predictive signature of R/R DLBCL has been yet identified to guide individualized risk-adapted therapy.[9]

In this context, we have previously shown that CYCLON, a nuclear germline factor, was acting as an autonomous tumor growth driver and anti-CD20 treatment resistance factor in DLBCL.[10] Little information is available about CYCLON function, besides its predominant expression in germ cells and induction in several high-proliferation contexts: cytokine-signaling,[11] regulation of T-cell immune homeostasis after cell activation[12] and as a Myc downstream target in murine antigen-dependent B cell differentiation.[13] Another intriguing feature of this protein is its entirely disordered structure, which suggest a function within phase-separated compartments.[14] Here, we describe how CYCLON subnuclear localization represents a novel potent prognostic marker for R-CHOP–treated DLBCL patients.

Ninety-seven R-CHOP–treated DLBCL patients were included in a bicentric retrospective cohort. Cohort characteristics are in full accordance with the literature (Table 1) with a near equal gender repartition and a median age of 67 years. More than half of the patients presented an advanced stage of the disease (Ann Arbor stage = III–IV or R-IPI score≥3). Median follow-up time, treatment details, survival, and response rates are detailed in Table 1. Hans' algorithm classification revealed that non-GC subtype (62.9%) was enriched compared with GC subtype (37.1%) and, as expected, associated with a worse prognosis (Supplemental Digital Content, Figure 1A, http://links.lww.com/HS/A164), similarly to the high risk R-IPI group (Supplemental Digital Content, Figure 1B, http://links.lww.com/HS/A164). More details about inclusion criteria, clinicobiological data, and cohort characteristics are given in Supplemental Digital Content, Methods, http://links.lww.com/HS/A163.

CYCLON immunohistochemistry (IHC) analysis was performed on tissue microarrays (TMA) under standard procedures using HPA041117 antibody (Atlas Antibodies) and independently reviewed by 2 expert pathologists as described in Supplemental Digital Content, Methods, http://links.lww.

[1]*Department of Cytology and Pathology, Grenoble-Alpes University Hospital, Grenoble, France*
[2]*Institute for Advanced Biosciences, INSERM U1209/CNRS UMR 5309/Grenoble Alpes University, Grenoble, France*
[3]*Department of Clinical Hematology, Grenoble-Alpes University Hospital, Grenoble, France*
[4]*Unit for Innovation in Genetics and Epigenetics in Oncology and Dijon University Hospital, University of Bourgogne, INSERM 1231, Dijon, France*
[5]*Hematology, Oncogenetics and Immunology Unit, Grenoble-Alpes University Hospital, Grenoble, France*
[6]*Daniel Hollard Institute, Grenoble, France*
[7]*Pole Recherche, Grenoble-Alpes University Hospital, Grenoble, France*
[*]*Current address for A. Bouroumeau: Division of Clinical Pathology, Diagnostic Department, Hopitaux Universitaires Genève, Geneva, Switzerland.*
Supplemental digital content is available for this article.

HemaSphere (2021) 5:7(e598). http://dx.doi.org/10.1097/HS9.0000000000000598.
Received: 8 February 2021 / Accepted: 4 May 2021

Table 1

Cohort Description.

Parameters	Value (Range) % [Proportion]
Median age at diagnosis (y)	67 (29–94)
>60	69.1% [67/97]
Gender	
Male	55.7% [54/97]
Female	44.3% [43/97]
Median follow-up time (mo)	41.1 (2–93, 95% CI, 29.0–53.6)
First-line therapy	
R-CHOP	80.4% [78/97]
+ Methotrexate	9.3% [9/97]
R-CHOP like	19.6% [19/97]
Mini R-CHOP	8.2% [8/97]
R-CVP	9.3% [9/97]
R-CHVP	1.0% [1/97]
R-COP	1.0% [1/97]
Complete response rate	78.3% [76/97]
Overall response rate	83.5% [81/97]
Primary refractory cases	20.6% [20/97]
Relapse cases	18.5% [18/97]
SOS	24 mo: 70.3% (95% CI, 59.4–78.8)
	60 mo: 62.0% (95% CI, 49.4–72.4)
	92 mo: 62.0% (95% CI, 49.4–72.4)
PFS	24 mo: 63.7% (95% CI, 52.9–72.7)
	60 mo: 55.7% (95% CI, 42.7–66.9)
	92 mo: 51.1% (95% CI, 36.2–64.1)
Ann Arbor staging classification (diagnosis)	
I (Single LN involves)	11.3% [11/97]
II (2 or more LN ipsilateral to the diaphragm)	20.6% [20/97]
III (LN on both sides of the diaphragm)	21.6% [21/97]
IV (involvement extralymphatic organs or tissues)	46.4% [45/97]
LDH > upper limit of normal	75.0% [73/97]
R-IPI class (diagnosis)	
Very low risk: 0	7.2% [7/97]
Low risk: 1–2	44.3% [43/97]
High risk: 3–5	48.5% [47/97]
DLBCL subtype (Hans' algorithm)	
GC	37.1% [36/97]
Non-GC	62.9% [61/97]
Genetics	
High grade B-cell lymphoma (double/triple hits)	3.1% [3/97]
MYC rearrangements	9.0% [8/89]
Including MYC-Ig	4.5% [4/89]
CYCLON (IHC pattern)	
Negative	7.2% [7/97]
Pan-nuclear	61.9% [60/97]
Nucleolar	12.4% [12/97]
Extranucleolar	18.6% [18/97]

DLBCL = diffuse large B-cell lymphoma; GC = germinal center; IHC = immunohistochemistry; LDH = lactate dehydrogenase; LN = lymph node; MYC-Ig = gene rearrangement involving MYC and Immunoglobulin loci; PFS = progression-free survival; R-CHOP = rituximab-cyclophosphamide, hydroxydaunorubicine, oncovin, prednisone; R-CHVP = rituximab-cyclophosphamide, hydroxydaunorubicine, vincristine, prednisone; R-COP = rituximab-cyclophosphamide, oncovin, prednisone; R-CVP = rituximab-cyclophosphamide, vincristine, prednisone; R-IPI = revised version of the International Prognostic Index; SOS = specific overall survival.

com/HS/A163). Reliability of positive cell rates and staining intensity scores between TMA cores was assessed using intraclass correlation coefficients (see Supplemental Digital Content, Methods, http://links.lww.com/HS/A163). CYCLON IHC showed a broad range of nuclear staining intensities and positive cells rates (Supplemental Digital Content, Figure 2, http://links.lww.com/HS/A164, left). Strikingly, it revealed 4 different and mutually exclusive aspects (Table 1; Figure 1A): negative (7/97), diffuse pan-nuclear (60/97), exclusively nucleolar (12/97), or extranucleolar staining (18/97) confirmed by AgNOR (Silver-Ag-staining of Nucleolar Organiser Regions) staining (Supplemental Digital Content, Figure 3, http://links.lww.com/HS/A164). High staining intensity (score 2–3), reflecting moderate/high CYCLON protein levels, was more frequently observed for nucleolar or extranucleolar cases (Supplemental Digital Content, Figure 2, http://links.lww.com/HS/A164, upper left panel) and was confirmed to be a robust criterion to distinguish them from pan-nuclear pattern using a multinomial regression model (Supplemental Digital Content, Table 1, http://links.lww.com/HS/A164).

While no significant differences in progression-free survival (PFS) or specific overall survival (SOS) were found between negative and positive CYCLON expression groups (Supplemental Digital Content, Figure 4A, http://links.lww.com/HS/A164), Kaplan-Meier survival analyses showed highly significant differences between CYCLON staining patterns for PFS ($P = 0.0015$) and SOS ($P = 0.0033$; Figure 1B). This was further supported by a log rank test for linear trend across CYCLON staining patterns ordered as negative, pan-nuclear, nucleolar, or extranucleolar (PFS: $P = 0.033$, SOS: $P = 0.023$). CYCLON extranucleolar ($CYCLON^{ex(+)}$) staining was clearly distinguishable from the other groups as patients in this group exhibit a high-risk profile. This was further supported by a multinomial classification model showing that the extranucleolar staining is more likely associated to primary refractory disease ($P < 0.001$) and relapse ($P = 0.026$) than nucleolar and pan-nuclear patterns (Supplemental Digital Content, Table 2, http://links.lww.com/HS/A164). The model showed that CYCLON extranucleolar staining was associated to refractory or relapse condition with equivalent probability (standard Wald test $P = 0.2$). CYCLON extranucleolar staining therefore clearly emerged as a marker of both primary refractory and relapse DLBCL. When comparing $CYCLON^{ex(+)}$ with $CYCLON^{ex(-)}$ category (including nucleolar, pan-nuclear, and negative staining patterns), the outcome of $CYCLON^{ex(+)}$ patients was, as expected, largely inferior to the outcome of $CYCLON^{ex(-)}$ patients for PFS ($P < 0.0001$) and SOS ($P = 0.0003$) when considering the whole cohort (Supplemental Digital Content, Figure 4B, http://links.lww.com/HS/A164). This was also observed for patients below 70 years treated with a full R-CHOP regimen (Supplemental Digital Content, Figure 4C, http://links.lww.com/HS/A164). Bootstrap resampling of Cox regression models for PFS and SOS confirmed the robustness of $CYCLON^{ex(+)}$ versus $CYCLON^{ex(-)}$ classification (Supplemental Digital Content, Table 3, http://links.lww.com/HS/A164). No association was found between CYCLON extranucleolar staining status (+/–) and GC/non-GC categories as shown by a standard χ^2 test ($P = 0.37$). The effect of GC versus non-GC on PFS and SOS was not influenced by the CYCLON extranucleolar (+/–) staining as demonstrated by Cox regression models including interaction terms (Supplemental Digital Content, Table 4, http://links.lww.com/HS/A164). Distribution of $CYCLON^{ex(+)}$ pattern does not significantly differ neither between patients treated with R-CHOP or R-CHOP like regimen (Supplemental Digital Content, Figure 4D, http://links.lww.com/HS/A164, χ^2 test $P = 0.725$) or patients below and above 70 years old (Supplemental Digital Content, Figure 4E, http://links.lww.com/HS/A164, χ^2 $P = 0.674$).

We next investigated whether CYCLON can act as applicable prognostic biomarker in the sense that its integration to R-IPI risk model and Hans' algorithm classification may improve identification of high-risk patients. Multivariate Cox models for PFS and SOS were built with $CYCLON^{ex(+)}$/$CYCLON^{ex(-)}$ categories, GC/non-GC subtypes and adjusted with the R-IPI score which was redistributed into 2 categories: low risk ($R\text{-}IPI^{(low)}$; 49 cases, IPI score 0–2) and high-risk ($R\text{-}IPI^{(high)}$; 48 cases, IPI score 3–5). As shown in Figure 1C, all 3 $CYCLON^{ex(+)}$, non-GC subtype, and $R\text{-}IPI^{(high)}$ categories were statistically significant and independent prognostic factors with strong negative impact on PFS and SOS. Hazard ratios were not statistically different

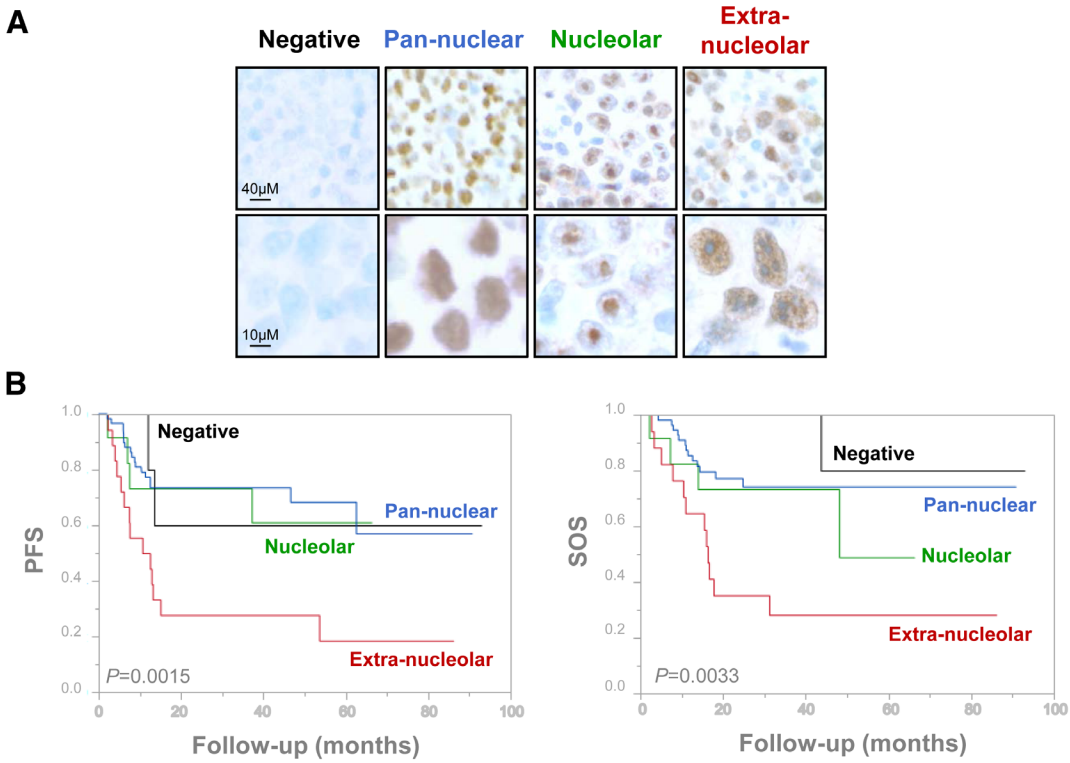

C

		PFS			SOS		
Variable	**Category**	**HR**	**95%CI***	***P***	**HR**	**95%CI***	***P***
CYCLON	$CYCLON^{ex(+)}$ versus $CYCLON^{ex(-)}$	2.74	1.29-5.83	0.003	2.7	1.12-6.52	0.008
R-IPI	$R\text{-}IPI^{(high)}$ versus $R\text{-}IPI^{(low)}$	3.05	1.4-6.63	0.003	3.77	1.52-9.31	0.002
HANS	non-GC versus GC	2.79	1.2-6.5	0.015	3.04	1.11-9.78	0.023

Figure 1. CYCLON subcellular localization define prognosis subgroups in DLBCL patients. (A), IHC analysis of CYCLON revealing distinct expression patterns in DLBCL patients as indicated. (B), Kaplan-Meier analyses of PFS (left) and SOS (right) associated to CYCLON patterns. *P* values are derived from a log-rank test. PFS, extranucleolar: 18.52% (95% CI, 3.98–41.4); nucleolar: 61.11% (95% CI, 25.46–83.75); diffuse: 56.91% (95% CI, 30.7–76.4); negative: 60% (95% CI, 12.57–88.18); SOS: extranucleolar: 31.11% (95% CI, 11.36–53.43); nucleolar: 48.89% (95% CI, 8.8–81); diffuse: 74.85% (95% CI, 60–84.75); negative: 80% (95% CI, 20.38–96.92). (C), Multivariate bootstrap Cox regression analyses of CYCLON extranucleolar staining status (+/–), R-IPI (high/low), and Hans' classification (GC/non-GC) for PFS and SOS. *Normal-approximation 95% CI based on bootstrap resampling (1000 replicates). Schoenfeld residual test, PFS model: global *P* = 0.58 and SOS model: global *P* = 0.72; Harrell's *C* statistic, PFS model: *C* = 0.72 and SOS model: *C* = 0.77. CI = confidence interval; DLBCL = diffuse large B-cell lymphoma; GC = germinal center; Hans = Hans algorithm defining non-GC and GC DLBCL subtypes; HR = hazard ratio; IHC = immunohistochemical; PFS = progression-free survival; R-IPI = revised version of the International Prognostic Index; SOS = specific overall survival.

for all 3 categories in PFS and SOS models as estimated by a standard Wald test ($P > 0.05$). Internal validation of Cox models stability was assessed by bootstrap resampling (Figure 1C and Supplemental Digital Content, Figure 5, http://links.lww.com/HS/A164). The prediction performance of the multivariate models did not depend markedly on follow-up time for PFS and SOS as assessed by ROC curves at 20, 40, 60, 80, 90 months with area under the curve ranging from 0.768 to 0.874 for PFS and 0.802 to 0.821 for SOS (Supplemental Digital Content, Figure 6, http://links.lww.com/HS/A164), indicating an end point-independent robust performance of PFS and SOS model predictions.

In view of the prognostic value of CYCLON staining patterns in DLBCL, we next asked whether this might correlate to specific genomic alterations. For this, we performed targeted next-generation sequencing of 48 DLBCL cases by using a 51-gene sequencing panel designed to reply to diagnosis, prognosis, and theranostic requirements in mature lymphoid neoplasms[15,16] (Supplemental Digital Content, Methods, http://links.lww.com/HS/A163; Supplemental Digital Content, Table 5, http://links.lww.com/HS/A164; and Supplemental Digital Content, Figure 7, http://links.lww.com/HS/A164). A Fisher exact test evaluating the association of each gene to CYCLON patterns revealed no statistically significant association between CYCLON patterns and mutational status for any of the 43 genes identified as mutated in this series according to our criteria. Given the broad diversity of DLBCL mutational profiles, this preliminary observation still warrants confirmation on a larger cohort. We also performed karyotyping and fluorescence in situ hybridization analyses of MYC, BCL2, and BCL6 loci, but we were not able to show any association of CYCLON extra-nucleolar pattern with HGBL subtype (all 3 cases presented a CYCLON pan-nuclear staining). Fisher exact test did not revealed statistically significant differences in CYCLON staining pattern distribution between MYC nonrearranged and rearranged cases (Fisher exact test $P = 0.1$,

Supplemental Digital Content, Figure 8A, http://links.lww.com/HS/A164). Of note, no case presenting both MYC rearrangement and CYCLON extranucleolar pattern could be detected in our series. A significant difference in CYCLON staining pattern distribution was observed between IHC MYC negative and positive cases (Fisher exact test $P = 0.001$, Supplemental Digital Content, Figure 8B, http://links.lww.com/HS/A164), but this is due to an excess of MYC-positive cases for the nucleolar pattern; MYC negative/positive cases being balanced for CYCLON extranucleolar pattern. From this limited set of data, CYCLON extranucleolar pattern therefore does not seem to correlate with any specific mutational or MYC expression profile.

In summary, this study reveals an extranucleolar CYCLON IHC staining pattern which, combined with R-IPI and GC/non-GC classifications, contributes substantially to identify adverse outcomes in R-CHOP–treated DLBCL. CYCLON IHC evaluation could be easily implemented in the clinical practice, as it would rely on standard automated procedure available in most centers involved in DLBCL management and provide a more precise discrimination of high-risk R-CHOP–treated DLBCL patients that could be eligible to risk-adapted strategies. Consistently with our previous findings[10] and based on IHC staining intensity (Supplemental Digital Content, Figure 2, http://links.lww.com/HS/A164 and Supplemental Digital Content, Table 1, http://links.lww.com/HS/A164), both CYCLON nucleolar and extranucleolar pattern could be related to higher expression levels of the protein, which would then accumulate either within or outside nucleoli. CYCLON being a highly phosphorylated unstructured protein, we could postulate that distinct phosphorylation events or protein/protein and protein/nucleic acid interactions within phase-separated compartments[14] might control these alternate localizations. Further investigations will be required to decipher the biological mechanisms that drive CYCLON exclusion from the nucleolus, its functional significance and association with aggressive clinical features, as well as to further validate its prognosis impact in a larger cohort.

Acknowledgments

We thank Dr Caroline Chapusot, PhD, and Dr Benjamin Tournier, PhD, for supervising next-generation sequencing (Dijon University Hospital).

Disclosures

The authors have no conflicts of interest to disclose.

Source of funding

This work is supported by research funding from ERiCAN (Epigenetic Reprogramming of Cancer cell plasticity and resilience) program of MSD AVENIR foundation (AE, S. Carras) and Grenoble University Hospital institutional grant (AE, TB, RG). MBC acknowledges funding from the Region Bourgogne-Franche-Comté-FEDER for the "ReHETLym" research program and the Fondation ARC.

References

1. Teras LR, DeSantis CE, Cerhan JR, et al. 2016 US lymphoid malignancy statistics by World Health Organization subtypes. *CA Cancer J Clin*. 2016;66:443–459.
2. Swerdlow SH, Campo E, Pileri SA, et al. The 2016 revision of the World Health Organization classification of lymphoid neoplasms. *Blood*. 2016;127:2375–2390.
3. Coiffier B, Thieblemont C, Van Den Neste E, et al. Long-term outcome of patients in the LNH-98.5 trial, the first randomized study comparing rituximab-CHOP to standard CHOP chemotherapy in DLBCL patients: a study by the Groupe d'Etudes des Lymphomes de l'Adulte. *Blood*. 2010;116:2040–2045.
4. Sehn LH, Berry B, Chhanabhai M, et al. The revised International Prognostic Index (R-IPI) is a better predictor of outcome than the standard IPI for patients with diffuse large B-cell lymphoma treated with R-CHOP. *Blood*. 2007;109:1857–1861.
5. Sarkozy C, Traverse-Glehen A, Coiffier B. Double-hit and double-protein-expression lymphomas: aggressive and refractory lymphomas. *Lancet Oncol*. 2015;16:e555–e567.
6. Rosenwald A, Wright G, Chan WC, et al; Lymphoma/Leukemia Molecular Profiling Project. The use of molecular profiling to predict survival after chemotherapy for diffuse large-B-cell lymphoma. *N Engl J Med*. 2002;346:1937–1947.
7. Schmitz R, Wright GW, Huang DW, et al. Genetics and pathogenesis of diffuse large B-cell lymphoma. *N Engl J Med*. 2018;378:1396–1407.
8. Wright GW, Huang DW, Phelan JD, et al. A probabilistic classification tool for genetic subtypes of diffuse large B cell lymphoma with therapeutic implications. *Cancer Cell*. 2020;37:551–568.e14.
9. Sehn LH, Gascoyne RD. Diffuse large B-cell lymphoma: optimizing outcome in the context of clinical and biologic heterogeneity. *Blood*. 2015;125:22–32.
10. Emadali A, Rousseaux S, Bruder-Costa J, et al. Identification of a novel BET bromodomain inhibitor-sensitive, gene regulatory circuit that controls rituximab response and tumour growth in aggressive lymphoid cancers. *EMBO Mol Med*. 2013;5:1180–1195.
11. Hoshino A, Fujii H. Redundant promoter elements mediate IL-3-induced expression of a novel cytokine-inducible gene, cyclon. *FEBS Lett*. 2007;581:975–980.
12. Saint Fleur S, Hoshino A, Kondo K, et al. Regulation of Fas-mediated immune homeostasis by an activation-induced protein, Cyclon. *Blood*. 2009;114:1355–1365.
13. Dominguez-Sola D, Victora GD, Ying CY, et al. The proto-oncogene MYC is required for selection in the germinal center and cyclic reentry. *Nat Immunol*. 2012;13:1083–1091.
14. Yoshizawa T, Nozawa RS, Jia TZ, et al. Biological phase separation: cell biology meets biophysics. *Biophys Rev*. 2020;12:519–539.
15. Dubois S, Viailly PJ, Mareschal S, et al. Next-generation sequencing in diffuse large B-cell lymphoma highlights molecular divergence and therapeutic opportunities: a LYSA study. *Clin Cancer Res*. 2016;22:2919–2928.
16. Sujobert P, Le Bris Y, de Leval L, et al. The need for a consensus next-generation sequencing panel for mature lymphoid malignancies. *HemaSphere*. 2019;3:e169.